

# Commodity Resource Valuation And Extraction: A Pathwise Programming Approach

Juri Hinz      Tanya Tarnopolskaya      Jeremy Yee\*

September 19, 2018

## Abstract

Complexity and uncertainty associated with commodity resource valuation and extraction requires stochastic control methods suitable for high dimensional states. Recent progress in duality and trajectory-wise techniques has introduced a variety of fresh ideas to this field with surprising results. This paper presents a first application of this promising development to commodity extraction problems. We introduce efficient algorithms for obtaining approximate solutions along with a diagnostic technique, which provides a quantitative measure for solution performance in terms of the distance between the approximate and the optimal control policy.

**Keywords** Duality, Markov decision process, natural resource extraction, optimal switching, real option, value function approximation

## 1 Introduction

Extraction projects for commodities and their valuation can often be formulated as optimal stochastic control problems of the switching type. Such problems usually have no known closed-form solutions and hence numerical methods often remain the only practical approach to address important operational and investment questions. This paper presents a family of novel methods for calculating approximate numerical solutions based on primal and dual techniques. While the primal methods are based on the so-called *convex stochastic switching* (CSS) and deliver an approximate solution, the dual methods utilize recent advances of *pathwise dynamic programming* to provide solution improvement and its quality assessment. This paper will demonstrate our algorithms by considering the optimal decision policy and value of natural resource assets associated with commodity extraction. Numerical results were obtained using the authors' software package implemented in the statistical language *R*. Similar optimal switching problems were considered by [2–4, 6, 16, 17]. This paper will depart from the standard literature and consider the presence of *mean reversion* in the commodity price, operational efficiencies in the form of *wasteful extraction*, *physical delivery* obligations to clients and commodity prices subject to *stochastic volatility*. These considerations add realism to our study and sheds practical insights.

In the next section, we introduce the problem setting. Section 3 outlines our numerical approach while Section 5 contains the numerical results. Section 6 concludes.

## 2 Commodity Extraction As A Stochastic Switching Problem

This paper will examine the management of a commodity resource with a finite amount of commodity as studied by [4]. In this setting, the decision maker aims to maximize the total expected profit using controls whose costs are given in Table 2.1. Doing so, the controller dynamically switches the operational mode of the resource between {Opened, Closed, Abandoned}. When opened, commodity is extracted, sold at the spot market and a revenue is realized based on the commodity price. While closed, commodity is preserved but a maintenance cost is incurred. The abandoned mode incurs no cost and provides no revenue. Switching to the abandoned mode causes the mode to remain permanently there. There is a switching cost between modes.

Table 2.1: Hypothetical Commodity Resource.

Output rate: 10 million pounds/year	Inventory level: 150 million pounds
Costs of production: \$0.50/pound	Opening/closing costs: \$200,000
Maintenance costs: \$500,000/year	Inflation rate: 8%/year
Convenience yield: 1%/year	Price variance: 8%/year
Real estate tax: 2%/year	Income tax: 50%
Royalty tax: 0%	Interest rate: 10%/year

The original problem setting in [4] was considered in a continuous time setting and solved using numerical partial differential equations. However, this paper will consider the problem as a *Markov decision process* (see [11]) in discrete time and a finite time horizon. The rates, costs and taxes above will be adjusted accordingly.

Given a finite time horizon  $\{0, 1, \dots, T\} \subset \mathbb{N}$ , consider a controlled Markovian process  $(X_t)_{t=0}^T := (P_t, Z_t)_{t=0}^T$  which consists of two parts. The discrete component  $(P_t)_{t=0}^T$  describes the evolution of a finite-state controlled Markov chain which takes values in a finite set  $\mathbf{P}$ . Further assume that at any time  $t = 0, \dots, T-1$  the controller takes an action  $a \in \mathbf{A}$  from a finite set  $\mathbf{A}$  of all admissible actions in order to cause the one-step transition from the mode  $p \in \mathbf{P}$  to the mode  $p' \in \mathbf{P}$  with a probability  $\alpha_{p,p'}(a)$ , where  $(\alpha_{p,p'}(a))_{p,p' \in \mathbf{P}}$  are pre-specified stochastic matrices for all  $a \in \mathbf{A}$ . Let us now turn to the evolution of the other component  $(Z_t)_{t=0}^T$  of the state process  $(X_t)_{t=0}^T$ . Here, we assume that it follows an uncontrolled evolution in the Euclidean space  $\mathbb{R}^d$  driven as

$$Z_{t+1} = W_{t+1}Z_t, \quad t = 0, \dots, T-1$$

by independent *disturbance matrices*  $(W_t)_{t=1}^T$ . That is, the transition kernels  $\mathcal{K}_t^a$  governing the evolution of our controlled Markov process  $(X_t)_{t=0}^T := (P_t, Z_t)_{t=0}^T$  from time  $t$  to  $t+1$  is given for each  $a \in \mathbf{A}$  by

$$\mathcal{K}_t v(p, z) = \sum_{p' \in \mathbf{P}} \alpha_{p,p'}(a) \mathbb{E}(v(p', W_{t+1}z)), \quad p \in \mathbf{P}, z \in \mathbb{R}^d, t = 0, \dots, T-1$$

which acts on each function  $v : \mathbf{P} \times \mathbb{R}^d \rightarrow \mathbb{R}$  where the above expectations are well-defined.

In this work, we use the discrete component  $(P_t)_{t=0}^T$  to convey information regarding the remaining level of commodity and the current operational mode. More

precisely, set  $\mathbf{P} = \{0, 1, \dots, I\} \times \{1, 2\}$  to capture all possible positions with the interpretation that the first component  $p^{(1)}$  of the position  $(p^{(1)}, p^{(2)}) \in \mathbf{P}$  describes the remaining commodity level such that  $p^{(1)} = 0$  represent an exhausted or abandoned resource. The second component  $p^{(2)}$  indicates whether the current operational mode is closed ( $p^{(2)} = 1$ ) or opened ( $p^{(2)} = 2$ ). To introduce the mode control, we set  $\mathbf{A} = \{0, 1, 2\}$  where  $a = 0, 1, 2$  stands for the action to abandon, to close, and to open the asset, respectively. The second component  $(Z_t)_{t=0}^T$  will be used to capture the market dynamics of the commodity price. The exact form of the disturbance matrices depends on the particular choice of the price process. If the system is in the state  $(p, z)$ , the costs of applying action  $a \in \mathbf{A}$  at time  $t = 0, \dots, T-1$  are expressed through  $r_t(p, z, a)$ . Having arrived at time  $t = T$  in the state  $(p, z)$ , a final *scrap value*  $r_T(p, z)$  is collected. Thereby the reward and scrap functions

$$r_t : \mathbf{P} \times \mathbb{R}^d \times \mathbf{A} \rightarrow \mathbb{R}, \quad r_T : \mathbf{P} \times \mathbb{R}^d \rightarrow \mathbb{R}$$

are exogenously given for  $t = 0, \dots, T-1$ . In our applications, the scrap value is

$$r_T(p, z) = \max_{a \in \mathbf{A}} r_T(p, z, a), \quad (p, z) \in \mathbf{P} \times \mathbb{R}^d$$

where the reward functions are specified in the following manner. If the asset is abandoned, there are neither costs nor revenue

$$r_t((0, p^{(2)}, z), a) = 0, \quad a \in \mathbf{A}, z \in \mathbb{R}^d.$$

For the case where  $p^{(1)} > 0$ , we define

$$r_t((p^{(1)}, p^{(2)}, z), a) = h_t(z)1_{\{2\}}(a) + m_t 1_{\{1\}}(a) + c_t 1_{\{1,2\}}(a) |p^{(2)} - a|$$

with the following interpretation: If the resource is opened, a revenue is collected which depends on continuous state component  $z$  through a pre-specified convex function  $h_t$ . If the resource is closed, then non-stochastic maintenance fee  $m_t$  is to be paid. Finally, a deterministic switching fee  $c_t$  is incurred whenever the operational mode transitions from opened to closed or vice versa. At each time  $t = 0, \dots, T$  the *decision rule*  $\pi_t$  is given by a mapping  $\pi_t : \mathbf{P} \times \mathbb{R}^d \rightarrow \mathbf{A}$ , prescribing at time  $t$  an action  $\pi_t(p, z) \in \mathbf{A}$  for a given state  $(p, z) \in \mathbf{P} \times \mathbb{R}^d$ . A sequence  $\pi = (\pi_t)_{t=0}^{T-1}$  of decision rules is called a *policy*. For each policy  $\pi = (\pi_t)_{t=0}^{T-1}$ , the so-called policy value  $v_0^\pi(p_0, z_0)$  is defined as the total expected reward

$$v_0^\pi(p_0, z_0) = \mathbb{E}^{(p_0, z_0), \pi} \left[ \sum_{t=0}^{T-1} r_t(P_t, Z_t, \pi_t(P_t, Z_t)) + r_T(P_T, Z_T) \right].$$

In this formula  $\mathbb{E}^{(p_0, z_0), \pi}$  stands for the expectation with respect to the probability distribution of  $(X_t)_{t=0}^T := (P_t, Z_t)_{t=0}^T$  induced by the Markov transitions from  $(P_t, Z_t)$  to  $(P_{t+1}, Z_{t+1})$  induced by the kernels  $\mathcal{K}_t^{\pi_t(P_t, Z_t)}$  for  $t = 0, \dots, T-1$ , given the initial value  $(P_0, Z_0) = (p_0, z_0)$ .

Now we turn to the optimization goal. A policy  $\pi^* = (\pi_t^*)_{t=0}^{T-1}$  is called optimal if it maximizes the total expected reward over all policies  $\pi \mapsto v_0^\pi(p, z)$ . To obtain such policy, one introduces for  $t = 0, \dots, T-1$  the so-called *Bellman operator*

$$\mathcal{T}_t v(p, z) = \max_{a \in \mathbf{A}} \left[ r_t(p, z, a) + \sum_{p' \in \mathbf{P}} \alpha_{p, p'}(a) \mathbb{E}[v(p', W_{t+1} z)] \right] \quad (2.1)$$

for  $(p, z) \in \mathbf{P} \times \mathbb{R}^d$ , acting on all functions  $v$  where the stochastic kernel is defined. Consider the *Bellman recursion*, also referred to as backward induction:

$$v_T(p, z) = r_T(p, z), \quad v_t = \mathcal{T}_t v_{t+1} \quad \text{for } t = T-1, \dots, 0. \quad (2.2)$$

Having assumed that the reward functions are convex and globally Lipschitz and the disturbances  $W_{t+1}$  are integrable, there exists a recursive solution  $(v_t^*)_{t=0}^T$  to the Bellman recursion ([7]). These functions  $(v_t^*)_{t=0}^T$  are called *value functions* and they determine an optimal policy  $\pi^* = (\pi_t^*)_{t=0}^T$  via

$$\pi_t^*(p, z) = \arg \max_{a \in \mathbf{A}} \left[ r_t(p, z, a) + \sum_{p' \in \mathbf{P}} \alpha_{p, p'}(a) \mathbb{E}[v_{t+1}^*(p', W_{t+1}z)] \right], \quad (2.3)$$

for  $t = T-1, \dots, 0$ .

### 3 Primal Approximate Solution

The first step in obtaining a numerical solution to the backward induction (2.2) is an appropriate discretization of the Bellman operator (2.1) to

$$\mathcal{T}_t^n v(p, z) = \max_{a \in \mathbf{A}} \left( r_t(p, z, a) + \sum_{p' \in \mathbf{P}} \alpha_{p, p'}(a) \sum_{k=1}^n \nu_{t+1}^n(k) v(p', W_{t+1}(k)z) \right)$$

where the probability weights  $(\nu_{t+1}^n(k))_{k=1}^n$  corresponds to the distribution sampling  $(W_{t+1}(k))_{k=1}^n$  of each disturbance  $W_{t+1}$ . In the resulting modified backward induction governed by  $v_t^n = \mathcal{T}_t^n v_{t+1}^n$ , the modified functions  $(v_t^n)_{t=0}^T$  need to be described by algorithmically tractable objects. Since the reward and scrap functions are convex in the continuous variable, these modified value functions are also convex and can be approximated by piecewise linear and convex functions. For this, introduce the so-called sub-gradient envelope  $\mathcal{S}_{\mathbf{G}^m} f$  of a convex function  $f : \mathbb{R}^d \rightarrow \mathbb{R}$  on a grid  $\mathbf{G}^m \subset \mathbb{R}^d$  with  $m$  points i.e.  $\mathbf{G}^m = \{g^1, \dots, g^m\}$

$$\mathcal{S}_{\mathbf{G}^m} f = \vee_{g \in \mathbf{G}^m} (\nabla_g f)$$

which is a maximum of the sub-gradients  $\nabla_g f$  of  $f$  on all grid points  $g \in \mathbf{G}^m$ . Using the sub-gradient envelope operator, define the double-modified Bellman operator as

$$\mathcal{T}_t^{m,n} v(p, z) = \mathcal{S}_{\mathbf{G}^m} \max_{a \in \mathbf{A}} \left( r_t(p, z, a) + \sum_{p' \in \mathbf{P}} \alpha_{p, p'}(a) \sum_{k=1}^n \nu_{t+1}^n(k) v(p', W_{t+1}(k)z) \right).$$

The corresponding backward induction

$$v_T^{m,n}(p, z) = \mathcal{S}_{\mathbf{G}^m} \max_{a \in \mathbf{A}} r_T(p, z, a), \quad p \in \mathbf{P}, z \in \mathbb{R}^d \quad (3.1)$$

$$v_t^{m,n}(p, z) = \mathcal{T}_t^{m,n} v_{t+1}^{m,n}(p, z), \quad t = T-1, \dots, 0. \quad (3.2)$$

yields the so-called double-modified value functions  $(v_t^{n,m})_{t=0}^T$ . Under appropriate assumptions (see [7]), the double-modified value functions converge uniformly to the true value functions almost surely on compact sets. These assumptions include the convexity and global Lipschitz continuity of the rewards, the integrability of all disturbances and some restrictions on the distribution sampling and grid density.

Since the double-modified value functions  $(v_t^{m,n})_{t=0}^T$  are piece-wise linear and convex, they can be expressed in a compact and appealing form using matrix representations. Note that any piecewise convex function  $f$  can be described by a matrix where each linear functional is represented by a row in the matrix. To denote this relation, let us agree on the following notation: Given a function  $f$  and a matrix  $F$ , we write  $f \sim F$  whenever  $f(z) = \max(Fz)$  holds for all  $z \in \mathbb{R}^d$ . Let us emphasize that the sub-gradient envelope operation  $\mathcal{S}_{\mathbf{G}^m}$  on a grid  $\mathbf{G}^m$  is reflected in terms of a matrix representative by a specific row-rearrangement operator

$$f \sim F \Leftrightarrow \mathcal{S}_{\mathbf{G}^m} f \sim \Upsilon_{\mathbf{G}^m}[F]$$

where the row-rearrangement operator  $\Upsilon_{\mathbf{G}^m}$  associated with  $\mathbf{G}^m = \{g^1, \dots, g^m\} \subset \mathbb{R}^d$  acts on matrix  $F$  with  $d$  columns as follows:

$$(\Upsilon_{\mathbf{G}^m} F)_{i,\cdot} = F_{\text{argmax}(Fg^i),\cdot} \quad \text{for all } i = 1, \dots, m. \quad (3.3)$$

For piecewise convex functions, the result of maximization, summation, and composition with linear mapping, followed by sub-gradient envelope can be obtained using their matrix representatives. More precisely, if  $f_1 \sim F_1$  and  $f_2 \sim F_2$  holds, then it follows that

$$\begin{aligned} \mathcal{S}_{\mathbf{G}^m}(f_1 + f_2) &\sim \Upsilon_{\mathbf{G}^m}(F_1) + \Upsilon_{\mathbf{G}^m}(F_2) \\ \mathcal{S}_{\mathbf{G}^m}(f_1 \vee f_2) &\sim \Upsilon_{\mathbf{G}^m}(F_1 \sqcup F_2) \\ \mathcal{S}_{\mathbf{G}^m}(f_1(W\cdot)) &\sim \Upsilon_{\mathbf{G}^m}(F_1 W) \end{aligned}$$

where  $W$  is an arbitrary  $d \times d$  matrix and the operator  $\sqcup$  stands for binding matrices by rows. Therefore, the backward induction (3.1) and (3.2) can be expressed in terms of the matrix representatives  $V_t^{m,n}(p)$  of the value functions  $v_t^{(m,n)}(p, z)$  for  $p \in \mathbf{P}$ ,  $z \in \mathbb{R}^d$  and  $t = 0, \dots, T$ . Since the double-modified backward induction involves maximization, summations and compositions with linear mappings applied to piecewise linear convex functions, it can be rewritten in terms of matrix operations which results in the following algorithm.

---

**Algorithm 3.1:** Convex Stochastic Switching Algorithm

---

```

1 for  $p \in \mathbf{P}$  do
2   |  $V_T^{m,n}(p) \leftarrow \Upsilon_{\mathbf{G}^m} \sqcup_{a \in \mathbf{A}} \mathcal{S}_{\mathbf{G}^m} r_T(p, \cdot, a)$ 
3 end
4 for  $t \in \{T-1, \dots, 0\}$  do
5   | for  $p \in \mathbf{P}$  do
6     |  $\tilde{V}_{t+1}^{m,n}(p) \leftarrow \sum_{k=1}^n \nu_{t+1}^n(k) \Upsilon_{\mathbf{G}^m} V_{t+1}^{m,n}(p) W_{t+1}(k)$ 
7     end
8     | for  $p \in \mathbf{P}$  do
9       |  $V_t^{m,n}(p) \leftarrow \Upsilon_{\mathbf{G}^m} \sqcup_{a \in \mathbf{A}} \left( \mathcal{S}_{\mathbf{G}^m} r_t(p, \cdot, a) + \sum_{p' \in \mathbf{P}} \alpha_{p,p'}(a) \tilde{V}_{t+1}^{m,n}(p') \right)$ 
10      end
11 end
```

---

The continuation value  $\tilde{V}_{t+1}^{m,n}(p)$  given by the sixth line in Algorithm 3.1 can be further approximated by recalling that the disturbances  $W_{t+1}$  are independently and

identically distributed across time. Through the use of a suitable nearest neighbour algorithm to construct permutation matrices, the conditional expectation on the sixth line can be approximated to save a significant amount of computational effort. For further details, we refer the interested reader to [8].

A candidate for a nearly optimal policy is given by

$$\pi_t^{m,n}(p, z) = \arg \max_{a \in \mathbf{A}} \left[ r_t(p, z, a) + \max_{p' \in \mathbf{P}} \left( \sum \alpha_{p,p'}(a) \tilde{V}_{t+1}^{m,n}(p')z \right) \right].$$

Given the pointwise convergence of the value functions for all  $p \in \mathbf{P}$ ,  $a \in \mathbf{A}$ , and  $t = 0, \dots, T-1$  one can deduce that

$$\lim_{(m,n) \rightarrow \infty} \pi_t^{m,n}(p, z) = \pi^*(p, z) \quad p \in \mathbf{P}, a \in \mathbf{A}, t = 0, \dots, T-1$$

holds for each point  $(p, z) \in \mathbf{P} \times \mathbb{R}^d$ . However, this convergence may be of little help in determining the quality of a candidate policy in practice. To address this issue, a pathwise dynamic approach will be described in the next subsection. This area has recently attracted growing research interest on diagnostics and potential a posteriori justification of an approximate control policy.

## 4 Dual Solution And Diagnostics

This section utilizes an approach suggested in [12] and [5] to assess the quality of a given control policy obtained by primal methods. Let us first illustrate their use for the case of an optimal stopping problem. Given a real-valued stochastic process  $(Z_t)_{t=0}^T$  adapted to a filtration, consider the family  $\mathcal{V}$  of all  $\{0, 1, \dots, T\}$ -valued stopping times. Obviously, the optimal stopping value is dominated

$$V_0^* = \sup_{\tau \in \mathcal{V}} \mathbb{E}(Z_\tau) \leq \mathbb{E}(\sup_{0 \leq t \leq T} Z_t)$$

by the expectation of the pathwise maximum. This dominance still holds

$$V_0^* = \sup_{\tau \in \mathcal{V}} \mathbb{E}(Z_\tau - M_\tau) \leq \mathbb{E}(\sup_{0 \leq t \leq T} (Z_t - M_t)).$$

when the original process  $(Z_t)_{t=0}^T$  is replaced by  $(Z_t - M_t)_{t=0}^T$  with a martingale  $(M_t)_{t=0}^T$  starting at the origin  $M_0 = 0$ . Furthermore, it turns out that this estimate is tight

$$V_0^* = \inf_{(M_t)_{t=0}^T} \mathbb{E}(\sup_{0 \leq t \leq T} (Z_t - M_t)) = \mathbb{E}(\sup_{0 \leq t \leq T} (Z_t - M_t^*)) \quad (4.1)$$

where the infimum is taken over the family of all martingales starting at the origin and in fact is attained at some *optimal martingale*  $(M_t^*)_{t=0}^T$  from this family. Usually, an optimal martingale is not available, as its knowledge is equivalent to the solution of the stopping problem. The equation (4.1) yields a practical way to estimate the optimal value  $V_0^*$  via a Monte Carlo procedure by determining an average of the pathwise maximum on a number of simulated trajectories of  $(Z_t - \tilde{M}_t)_{t=0}^T$ . Obviously, to obtain a tight upper estimate, the martingale  $(\tilde{M}_t)_{t=0}^T$  must resemble the optimal one. Similarly, a lower estimate for  $V_0^*$  can be obtained from Monte-Carlo average of independent realizations of  $Z_{\tilde{\tau}} - \tilde{M}_{\tilde{\tau}}$ , based on an arbitrary stopping time  $\tilde{\tau}$ . Again to obtain a tight lower bound, the stopping time  $\tilde{\tau}$  must be chosen close to the optimal

stopping time. This procedure of bound estimate exhibits an interesting self-tuning property: The closer  $(\tilde{M}_t)_{t=0}^T$  and  $\tilde{\tau}$  are to their optimal counterparts, the lower the variance of the Monte-Carlo trials and the narrower the gap between both bounds. In a hypothetic case where  $\tilde{\tau}$  is the optimal stopping time and  $(\tilde{M}_t)_{t=0}^T$  is the optimal martingale, the variance of both Monte-Carlo tails reduces to zero. Moreover, in this case the upper and the lower bounds coincide with the optimal stopping value.

This approach has been successfully applied [1] and generalized to multiple stopping problems in finance [9]. For our switching problem, the pathwise dynamic programming approach works similarly (see [8]). Given an approximate control problem solution, two random bound variables are constructed, whose expectations give a lower and an upper estimate for the unknown value function. These bound variables are determined through a stochastic recursive procedure similar to the backward induction. Their calculation is effected in terms of a Monte-Carlo procedure whose in-sample empirical variance can be used to quote a confidence interval for the unknown value function. In this setting, the self-tuning property states that both, the variance of the Monte-Carlo trials and the gap between expectations of bound variables decrease, if the *approximate control policy* approaches the optimal policy.

Suppose that our numerical scheme returns approximate value functions  $(v_t)_{t=0}^T$  along with the approximate expected value functions  $(v_t^E)_{t=0}^T$ , thus we introduce an approximately-optimal policy  $\pi = (\pi_t)_{t=0}^{T-1}$  by

$$\pi_t(p, z) = \operatorname{argmax}(r_t(p, z, a) + \sum_{p' \in \mathbf{P}} \alpha_{p, p'}(a) v_{t+1}^E(p', z))$$

To answer the question how far is the strategy  $\pi$  from an optimal strategy  $\pi^*$ , we estimate the performance gap  $[v_0^\pi(p_0, z_0), v_0^{\pi^*}(p_0, z_0)]$  at a given point  $(p_0, z_0) \in \mathbf{P} \times \mathbb{R}^d$  by an explicit construction of random variables  $\underline{v}_0^{\pi, \varphi}(p_0, z_0)$ ,  $\bar{v}_0^\varphi(p_0, z_0)$  satisfying

$$\mathbb{E}(\underline{v}_0^{\pi, \varphi}(p_0, z_0)) = v_0^\pi(p_0, z_0) \leq v_0^{\pi^*}(p_0, z_0) \leq \mathbb{E}(\bar{v}_0^\varphi(p_0, z_0)).$$

Using Monte-Carlo simulations, one estimates both means along with empirical confidence intervals to estimate the performance gap, which is narrow if the approximate solution is close to optimal. This useful property is due to the self-tuning property, which ensures that the more optimal solutions  $(v_t)_{t=0}^T$   $(v_t^E)_{t=0}^T$  return narrower gaps and lower variance in the Monte-Carlo scheme. This scheme can be implemented as follows

1. Given approximate solution  $(v_t)_{t=0}^T$   $(v_t^E)_{t=0}^T$  with the corresponding policy  $(\pi_t)_{t=0}^{T-1}$ , implement control variables  $(\varphi_t)_{t=1}^T$  as

$$\varphi_t(p, z, a) = \sum_{p' \in \mathbf{P}} \alpha_{p, p'}(a) \left( \frac{1}{I} \sum_{i=1}^I v_t(p', W_t^{(i)} z) - v_t(p', W_t z) \right),$$

for all  $p \in \mathbf{P}$ ,  $a \in \mathbf{A}$ ,  $z \in \mathbb{R}^d$ , where  $(W_t^{(1)}, \dots, W_t^{(I)}, W_t)_{t=1}^T$  are independent and  $(W_t^{(1)}, \dots, W_t^{(I)}, W_t)$  are identically distributed for each  $t = 1, \dots, T$ .

2. Chose a number  $K \in \mathbb{N}$  of Monte-Carlo trials and obtain for  $k = 1, \dots, K$  independent realizations  $(W_t(\omega_k))_{t=1}^T$  of disturbances.
3. Starting at  $z_0^k := z_0 \in \mathbb{R}^d$ , define for  $k = 1, \dots, K$  trajectories  $(z_t^k)_{t=0}^T$  recursively

$$z_{t+1}^k = W_{t+1}(\omega_k) z_t^k, \quad t = 0, \dots, T-1$$

and determine realizations

$$\varphi_t(p, z_{t-1}^k, a)(\omega_k), \quad t = 1, \dots, T, \quad k = 1, \dots, K.$$

4. For each  $k = 1, \dots, K$  initialize the recursion at  $t = T$  as

$$\underline{v}_T^{\pi, \varphi}(p, z_T^k)(\omega_k) = \overline{v}_T^{\pi}(p, z_T^k)(\omega_k) = r_T(p, z_T^k) \quad \text{for all } p \in \mathbf{P}$$

and continue for  $t = T - 1, \dots, 0$  and for all  $p \in \mathbf{P}$  by

$$\begin{aligned} \underline{v}_t^{\pi, \varphi}(p, z_t^k)(\omega_k) &= r_t(p, z_t^k, \pi_t(p, z_t^k)) + \varphi_{t+1}(p, z_t^k, \pi_t(p, z_t^k))(\omega_k) \\ &\quad + \sum_{p' \in \mathbf{P}} \alpha_{p, p'}(\pi_t(p, z_t^k)) \underline{v}_{t+1}^{\pi, \varphi}(p', z_{t+1}^k)(\omega_k) \\ \overline{v}_t^{\pi, \varphi}(p, z_t^k)(\omega_k) &= \max_{a \in \mathbf{A}} [r_t(p, z_t^k, a) + \varphi_{t+1}(p, z_t^k, a)(\omega_k)] \\ &\quad + \sum_{p' \in \mathbf{P}} \alpha_{p, p'}(a) \overline{v}_{t+1}^{\pi, \varphi}(p', z_{t+1}^k)(\omega_k) \end{aligned}$$

5. Calculate sample means  $\frac{1}{K} \sum_{k=1}^K \underline{v}_0^{\pi, \varphi}(p_0, z_0)(\omega_k)$ ,  $\frac{1}{K} \sum_{k=1}^K \overline{v}_0^{\pi, \varphi}(p_0, z_0)(\omega_k)$  to estimate the means  $\mathbb{E}(\underline{v}_0^{\pi, \varphi}(p_0, z_0))$ ,  $\mathbb{E}(\overline{v}_0^{\pi, \varphi}(p_0, z_0))$  along with their confidence intervals. These means will be referred to as the *primal* and *dual* values, respectively.

## 5 Numerical Results

This section demonstrates our algorithms on the commodity extraction problem described in Section 2. The values given by Table 2.1 will be adjusted in order fit our discrete time setting with time step  $\Delta = 0.25$  years between the decision times  $\{0, \dots, T\} \subset \mathbb{N}$  representing a time horizon  $[0, \bar{T}] = [0, 30]$  of thirty years, with four decisions made every year. Let us discretize the commodity levels remaining in the resource with the step size corresponding to commodity amount extracted within one time step  $\Delta$ . That is, the first entry of the discrete component covers the range  $p^{(1)} \in \{0, 1, \dots, \frac{\bar{p}}{\Delta}\}$  where  $\bar{p} = 15$  stands for the minimum number of years it takes to deplete the resource. Further, define the number of decision epochs  $T = \frac{\bar{T}}{\Delta} + 1$ , the maintenance costs  $m_t = m_0 \Delta e^{(\rho - r - \zeta)t\Delta}$  and the switching costs  $c_t = c_0 e^{(\rho - r - \zeta)t\Delta}$  with coefficients  $r = 0.1$ ,  $\rho = 0.08$ ,  $\zeta = 0.02$ ,  $m_0 = 0.5$  and  $c_0 = 0.2$  standing for the interest rate, rate of inflation, real estate tax, initial maintenance cost and initial switching cost, respectively.

**Geometric Brownian Motion:** Following [4], the continuous state component  $(Z_t)_{t=0}^T$  is one-dimensional and follows linear state dynamics:

$$Z_{t+1} = \exp\left(\left(\mu - \frac{\sigma^2}{2}\right)\Delta + \sigma\sqrt{\Delta}N_{t+1}\right) Z_t \quad (5.1)$$

with  $\sigma^2 = 0.08$  and independent identically standard normally distributed  $(N_t)_{t=1}^T$ . The controlled transition probabilities of the discrete component given  $(p^{(1)}, p^{(2)}) \in \mathbf{P}$  is uniquely determined by

$$\begin{aligned} \alpha_{(p^{(1)}, p^{(2)}), (\max\{p^{(1)} - 1, 0\}, \text{Opened})}(\text{Open}) &= 1, \\ \alpha_{(p^{(1)}, p^{(2)}), (p^{(1)}, \text{Closed})}(\text{Close}) &= 1, \\ \alpha_{(p^{(1)}, p^{(2)}), (0, p^{(2)})}(\text{Abandon}) &= 1. \end{aligned}$$



The mode is controlled deterministically under the above specification. Now let us define the control costs by a function, representing the revenue of the opened resource

$$h_t(z) = 5\Delta z e^{-(r+\zeta)t\Delta} - 2.5\Delta e^{(\rho-r-\zeta)t\Delta}$$

where the variable  $z$  represents the commodity price.

An equally spaced grid ranging from 0 to 20 of size 4,001 was used and a distribution sampling of size 20,000 constructed using equidistant sampling of standard normal quantiles was applied to obtain the following results. Table 5.1 lists the primal and dual values, generated using  $K = 1,000$  paths and  $I = 1,000$  sub-simulations. To compare our results with [4] listed in the first column of the Table 5.1, we assumed a convenience yield  $d = 0.01$  and set  $\mu = r - d = 0.09$  in (5.1). We were able to obtain similar results despite [4] using a continuous time formulation. Further, our results were able to obtain excellent precision as evidenced by the tight bounds and low standard errors given in the paranthesis.

Table 5.1: Resource Valuation Under Geometric Brownian Motion

$Z_0$	B&S		Opened Resource		Closed Resource	
	Open	Closed	Primal	Dual	Primal	Dual
0.3	1.25	1.45	1.2127(.0026)	1.2156(.0026)	1.4127(.0026)	1.4156(.0026)
0.4	4.15	4.35	4.1059(.0034)	4.1086(.0034)	4.3059(.0034)	4.3086(.0034)
0.5	7.95	8.11	7.9026(.0039)	7.9053(.0039)	8.0752(.0041)	8.0777(.0041)
0.6	12.52	12.49	12.5129(.0042)	12.5153(.0042)	12.4787(.0045)	12.4813(.0045)
0.7	17.56	17.38	17.5869(.0047)	17.5889(.0047)	17.3869(.0047)	17.3904(.0048)
0.8	22.88	22.68	22.9475(.0052)	22.9489(.0052)	22.7475(.0052)	22.7489(.0052)
0.9	28.38	28.18	28.4940(.0057)	28.4957(.0057)	28.2940(.0057)	28.2957(.0057)
1.0	34.01	33.81	34.1667(.0062)	34.1681(.0062)	33.9667(.0062)	33.9681(.0062)

This paper will illustrate the control policies in the form of the curves depicted in Figure 5.1. We have observed that for all the situations examined in this paper, the optimal policies share this structure. Namely, it is optimal to operate an open resource when the commodity price is sufficiently high. Below some price level, the resource should be shut down, either to the closed or abandoned mode. Typically, we have a curve bifurcation and the area between both curve branches represents the price range where switching to the closed mode is optimal. In the right plot of Figure 5.1, the optimal policies for a closed resource is shown for different values of  $\mu$ . Recall that there is a strong element of scarcity in our problem. That is, selling a unit of limited commodity now means that the same unit of commodity cannot be sold at a future date. Thus, we observe from Figure 5.1, that the decision maker is more willing to preserve commodity for future use if the drift term  $\mu$  is high. In our subsequent studies, we will assume drift  $\mu = r - d = 0.09$  (unless otherwise stated) in order to stay in line with [4].

**Ornstein-Uhlenbeck Process:** Commodity prices often mimic the business cycle in practice (see [10,14]). Prices with significant mean reversion often lead to different optimal behavior compared to those following geometric Brownian motions ([13–15]). To examine the impact of mean reversion, the logarithm of the commodity price  $(\log \tilde{Z}_t)_{t=0}^T$  is assumed to follow an AR(1) process, an auto-regression of order one. With this choice, define the linear state evolution  $(Z_t)_{t=0}^T$  in the required form

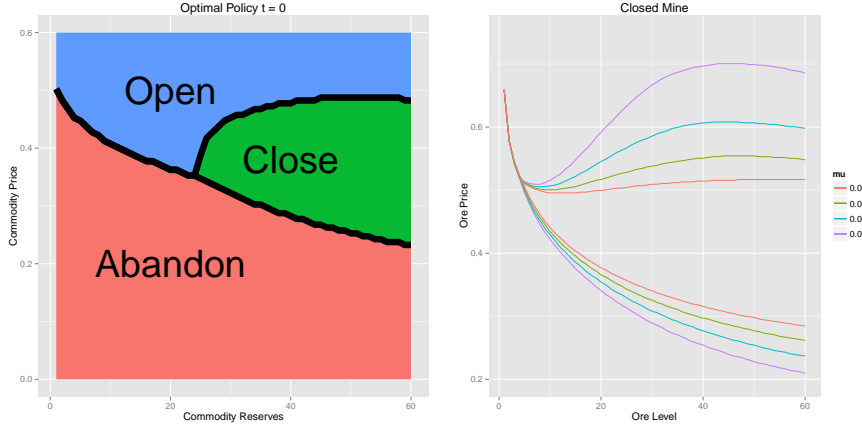


Figure 5.1: The optimal policy at  $t = 0$ . The horizontal axis represents remaining reserves while the vertical represents the commodity price. The right plot displays policy for a commodity resource that begins closed for  $\mu = 0.09, 0.08, 0.07, 0.06$ .

$Z_{t+1} = W_{t+1}Z_t$  as

$$Z_{t+1} := \begin{bmatrix} 1 \\ \log \tilde{Z}_{t+1} \end{bmatrix} = \begin{bmatrix} 1 & 0 \\ \left(\mu - \frac{\sigma^2}{2}\right)\Delta + \sigma\sqrt{\Delta}N_{t+1} & \phi \end{bmatrix} \begin{bmatrix} 1 \\ \log \tilde{Z}_t \end{bmatrix},$$

for  $t = 0, \dots, T - 1$ , with initial value  $\log \tilde{Z}_0 \in \mathbb{R}$  and  $\mu = 0.09$ ,  $\sigma^2 = 0.08$ . Again,  $(N_t)_{t=1}^T$  are independent standard normally distributed random variables and the parameter  $\phi \in [0, 1]$  determines the speed of mean reversion, where  $\phi = 1$  gives a geometric Brownian motion. Using the same parameters as before, merely adjust the cash flow function accordingly for  $t = 0, \dots, T - 1$  to

$$h_t(z) = 5\Delta \exp\left(z^{(2)}\right) \exp(-(r + \zeta)t\Delta) - 2.5\Delta \exp((\rho - r - \zeta)t\Delta)$$

since now the variable  $z^{(2)}$  captures the logarithmic commodity price. Figure 5.2 shows the nearly-optimal policies at initial time  $t = 0$  for an opened asset, which are computed using 2000 equally spaced grid points ranging from  $-5$  to  $5$  for  $\log(\tilde{Z}_t)$  and 10,000 disturbances constructed from the equidistant quantiles of the normal distribution. Diagnostics is performed using  $K = 500$  sample paths and  $I = 500$  sub-simulations. Table 5.2 contains results for  $\phi = 1, 0.8, 0.6$  and shows very tight bounds and low standard errors.

Figure 5.2 provides an interesting insight. We observe that under mean reversion  $|\phi| < 1$ , each additional unit of commodity reserve exhibit diminishing marginal value which directly contrasts the behaviour under geometric Brownian motion. This phenomenon was also observed for the closed commodity resource and will have significant implications later on.

**Wasteful Extraction:** For  $w \in [0, 1]$  and commodity level  $p^{(1)}$ , assume that

Table 5.2: Mean Reversion On Commodity Resource Valuation

$\phi$	$\tilde{Z}_0$	Opened Resource		Closed Resource	
		Primal	Dual	Primal	Dual
1	0.3	1.2198(.0047)	1.2278(.0049)	1.4198(.0049)	1.4279(.0049)
	0.4	4.1153(.0067)	4.1203(.0067)	4.3153(.0067)	4.3203(.0067)
	0.5	7.9133(.0074)	7.9179(.0075)	8.0863(.0078)	8.0900(.0078)
0.8	0.3	6.3187(.0006)	6.3189(.0006)	6.3027(.0006)	6.3029(.0006)
	0.4	7.2752(.0006)	7.2753(.0006)	7.0822(.0006)	7.0823(.0006)
	0.5	8.1160(.0006)	8.1161(.0006)	7.9160(.0006)	7.9161(.0006)
0.6	0.3	7.6732(.0003)	7.6733(.0003)	7.6034(.0003)	7.6034(.0003)
	0.4	8.1514(.0003)	8.1515(.0003)	7.9535(.0003)	7.9536(.0003)
	0.5	8.5754(.0003)	8.5755(.0003)	8.3754(.0003)	8.3755(.0003)

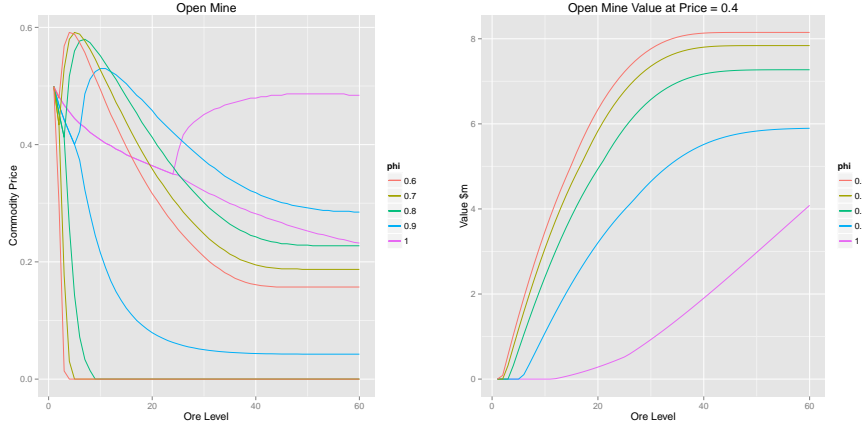


Figure 5.2: Left plot shows policy for an opened commodity resource under  $\phi = 1, 0.9, 0.8, 0.7, 0.6$  while the right displays the value of the resource as a function of commodity reserves for  $\tilde{Z}_0 = 0.4$ .

transition to the new position is now governed by the probabilities

$$\begin{aligned}
 \alpha_{(p^{(1)}, p^{(2)}), (\max\{p^{(1)}-2, 0\}, \text{Opened})}(\text{Open}) &= w \\
 \alpha_{(p^{(1)}, p^{(2)}), (\max\{p^{(1)}-1, 0\}, \text{Opened})}(\text{Open}) &= 1 - w \\
 \alpha_{(p^{(1)}, p^{(2)}), (p^{(1)}, \text{Closed})}(\text{Close}) &= 1 \\
 \alpha_{(p^{(1)}, p^{(2)}), (0, p^{(2)})}(\text{Abandon}) &= 1
 \end{aligned}$$

and zero otherwise, i.e. there is a probability  $w$  of wasting 1 additional unit of the commodity when the resource is in the opened mode.

The linear state evolution for  $(Z_t)_{t=0}^T$ , the cash flow  $h_t$ , the grid and the disturbance sampling of the disturbances from the Ornstein-Uhlenbeck process study will be reused to generate the results in this part. The primal and dual values in Table 5.3 were generated using  $K = 500$  sample paths and  $I = 500$  sub-simulations. As

Table 5.3: Commodity Resource Valuation Under Wastage

$\phi$	$w$	$\tilde{Z}_0$	Opened Resource		Closed Resource	
			Primal	Dual	Primal	Dual
1	0	0.3	1.2070(.0052)	1.2129(.0052)	1.4070(.0052)	1.4129(.0052)
		0.4	4.0989(.0071)	4.1020(.0071)	4.2989(.0071)	4.3020(.0071)
		0.5	7.8935(.0081)	7.9015(.0082)	8.0660(.0085)	8.0720(.0085)
0.5	0.3	0.3	0.1987(.0032)	0.2042(.0030)	0.3987(.0032)	0.4040(.0030)
		0.4	1.9322(.0047)	1.9352(.0048)	2.1322(.0047)	2.1352(.0048)
		0.5	4.5048(.0051)	4.5094(.0051)	4.6702(.0056)	4.6741(.0055)
0.6	0	0.3	7.6727(.0003)	7.6728(.0003)	7.6028(.0003)	7.6029(.0003)
		0.4	8.1509(.0003)	8.1510(.0003)	7.9530(.0003)	7.9531(.0003)
		0.5	8.5749(.0004)	8.5750(.0004)	8.3749(.0004)	8.3750(.0004)
0.5	0.3	0.3	7.6514(.0003)	7.6515(.0003)	7.5897(.0003)	7.5897(.0003)
		0.4	8.1296(.0003)	8.1296(.0003)	7.9393(.0003)	7.9393(.0003)
		0.5	8.5536(.0003)	8.5536(.0003)	8.3536(.0003)	8.3536(.0003)

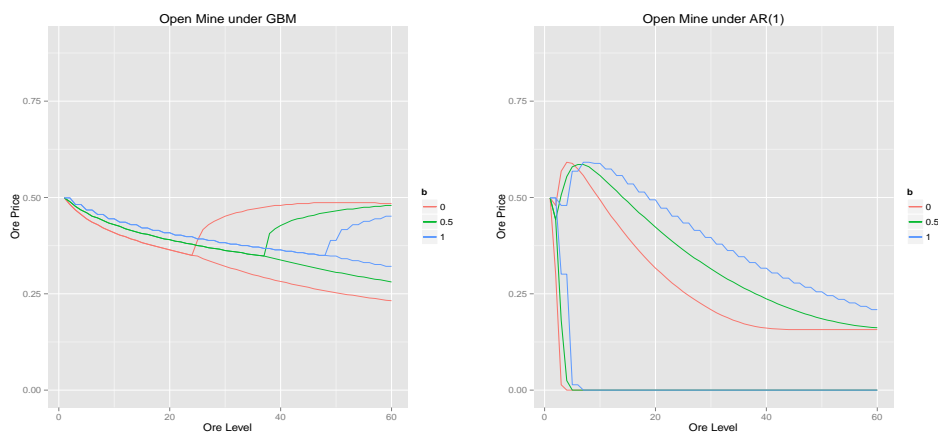


Figure 5.3: Optimal policies at  $t = 0$  for an opened resource under  $w = 0, 0.5, 1$ . The policies under  $\phi = 1$  are depicted on the left while the right shows  $\phi = 0.6$ .

usual, the bounds obtained are tight with low standard errors. Table 5.3 suggests that wasteful extraction has a minimal impact on the resource value when the price follows strong mean reversion ( $\phi = 0.6$ ) compared to geometric Brownian motion for our prices starting at  $\tilde{Z}_0$ . This may be directly related to the phenomenon observed earlier regarding the marginal value of each additional unit of the commodity. The impact on the optimal policies are shown in Figure 5.3 for  $w = 0, 0.5, 1$ .

**Physical Delivery:** Another prominent feature of commodity markets is the use of physical delivery contracts between suppliers and buyers. The reward function is modified in the following manner to incorporate this. If the asset is abandoned, there

are neither costs nor revenue

$$r_t((0, p^{(2)}, z), a) = 0, \quad a \in \mathbf{A}, z \in \mathbb{R}$$

For the case where  $p^{(1)} > 0$ , we have

$$r_t((p^{(1)}, p^{(2)}, z), a) = h_t(z)1_{\{2\}}(a) + m_t 1_{\{1\}}(a) + c_t 1_{\{1,2\}}(a)|p^{(2)} - a| - \psi_t(p^{(1)}, z)$$

where the values of  $m_t, c_t$  are already specified before and  $\psi_t$  represents the penalty function for deviating from the contract. This paper will consider penalty functions  $\psi : \mathbf{P} \times \mathbb{R}^2 \rightarrow \mathbb{R}$  of the form

$$\psi_t(p, z) = \begin{cases} b \exp(z^{(2)})(p^{(1)} - p_t^*), & \text{if } p^{(1)} > p_t^*; \\ 0 & \text{otherwise} \end{cases}$$

where  $z^{(2)}$  is the log commodity price,  $b \geq 0$  and  $p_0^{(1)} - p_t^*$  is the minimum amount of commodity that needs to be delivered by time  $t$  according to the contract. If this condition is not feasible, then the decision maker will need to compensate the buyer with a money amount equal to a proportion  $b$  of the current market value of the shortfall.

Table 5.4: Resource Valuation Under Physical Delivery Contracts

$\phi$	$b$	$\tilde{Z}_0$	Opened Resource		Closed Resource	
			Primal	Dual	Primal	Dual
1	0	0.3	1.2070(.0052)	1.2129(.0052)	1.4070(.0052)	1.4129(.0052)
		0.4	4.0989(.0071)	4.1020(.0071)	4.2989(.0071)	4.3020(.0071)
		0.5	7.8935(.0081)	7.9015(.0082)	8.0660(.0085)	8.0720(.0085)
	1	0.3	0.3133(.0036)	0.3169(.0035)	0.3703(.0036)	0.3752(.0035)
		0.4	3.0951(.0056)	3.1004(.0056)	2.9738(.0057)	2.9791(.0057)
		0.5	7.2354(.0070)	7.2395(.0070)	7.0435(.0071)	7.0496(.0071)
0.6	0	0.3	7.6727(.0003)	7.6728(.0003)	7.6028(.0003)	7.6029(.0003)
		0.4	8.1509(.0003)	8.1510(.0003)	7.9530(.0003)	7.9531(.0003)
		0.5	8.5749(.0004)	8.5750(.0004)	8.3749(.0004)	8.3750(.0004)
	1	0.3	7.6727(.0003)	7.6728(.0003)	7.5997(.0003)	7.5998(.0003)
		0.4	8.1509(.0003)	8.1510(.0003)	7.9529(.0003)	7.9530(.0003)
		0.5	8.5749(.0004)	8.5750(.0004)	8.3749(.0004)	8.3750(.0004)

The transition rule for  $(Z_t)_{t=0}^T$  and the cashflow  $h_t$  from the previous part will be reused, as well as the grid and the distribution sampling. The results in Table 5.4 were generated using  $b = 0, 1$ ,  $\phi = 1, 0.6$  and  $w = 0$ . We set

$$p_t^* = \begin{cases} p_0^{(1)} - \frac{3}{4}(t-1) & \text{for } t = 5, 9, 13, \dots, 41; \\ p_0^{(1)} & \text{otherwise} \end{cases}$$

where  $p_0^{(1)}$  is the starting commodity level. Under the above specification of  $p_t^*$ , the resource is contracted to deliver 3 units of the commodity by the first year, 6 units by the second year, ..., and 30 units by the end of the first decade. Using  $K = 500$  sample paths and  $I = 500$  sub-simulations in the diagnostics returns tight bounds and small standard errors, which are given in the parenthesis.

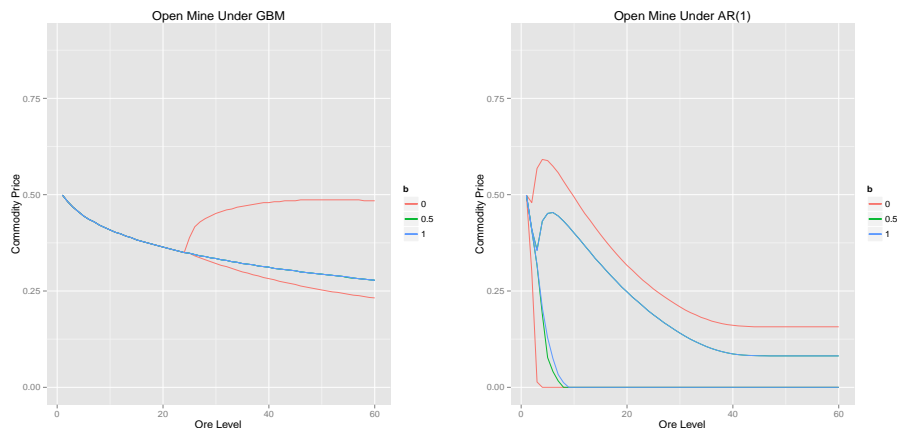


Figure 5.4: Optimal policy at  $t = 0$  under different values of  $b = 0, 0.5, 1$ . The policies under  $\phi = 1$  are depicted on the left while the right shows  $\phi = 0.6$ . Here the blue and green curves are almost identical.

In Table 5.4, physical delivery obligations seem to have little effect under strong mean reverting prices. In contrast, there is a significant impact under geometric Brownian motion prices. This can also be seen in the optimal policies for an opened resource at  $t = 0$ , as depicted in Figure 5.2.

**GARCH-type Process:** Such process are popular in modeling the effects of time-changing fluctuation intensity, the so-called volatility. However, the original GARCH definition includes non-linear recursion and is not covered by our approach which requires a linear state dynamics. For this reason, we suggest a simple modification in order to retain this characteristic feature. In what follows, we consider a GARCH(1,1)-like model. Having assumed the controlled operation mode dynamics  $(P_t)_{t=0}^T$  as in the original geometric Brownian motion case and the absence of any delivery contracts, we define the process  $(\log \tilde{Z}_t)_{t=0}^T$  recursively using independent standard normally distributed random variables  $(N_t)_{t=1}^T$  as

$$\begin{aligned}\sigma_{t+1}^2 &= \sigma^2 \beta + \beta_1 \sigma_t^2 + \beta_2 Y_t^2 \\ Y_{t+1}^2 &= \sigma_{t+1}^2 N_t^2 \\ \log(\tilde{Z}_{t+1}) &= \kappa \Delta + \phi \log(\tilde{Z}_t) + \sigma_{t+1}^2 \sqrt{\Delta} N_{t+1}\end{aligned}$$

for  $t = 0, \dots, T-1$ , with initial values  $\sigma_0^2 = \sigma^2 = \sqrt{0.08} Y_0^2$ ,  $\tilde{Z}_0 \in \mathbb{R}_+$  and parameters  $\kappa = \mu - \sigma^4/2 = 0.05$ ,  $\beta_1, \beta_2 \in \mathbb{R}_+$  with  $\beta_1 + \beta_2 \in [0, 1]$  such that  $\beta = 1 - \beta_1 - \beta_2$ . With this definition,  $(\sigma_t^2)_{t=0}^T$  follows the same recursion as the conditional variance the original GARCH(1,1) process and can be interpreted as the volatility proxy of the commodity price  $(\tilde{Z}_t)_{t=0}^T$  since  $\sigma_{t+1}^2 \sqrt{\Delta}$  is the conditional standard deviation of the increment  $\log \tilde{Z}_{t+1} - \log \tilde{Z}_t$  for  $t = 0, \dots, T-1$ . Positive values of  $\beta_1, \beta_2$  induces volatility clustering and a mean reversion is induced when  $\phi \in ]0, 1[$ . With this choice, we define the linear state evolution  $(Z_t)_{t=0}^T$  for the state variables

$$Z_t = [ 1, \sigma_t^2, Y_t^2, \log \tilde{Z}_t, ]^\top, \quad t = 0, \dots, T$$

in the required form  $Z_{t+1} = W_{t+1}Z_t$  as

$$Z_{t+1} = \begin{bmatrix} 1 & 0 & 0 & 0 \\ \sigma^2\beta & \beta_1 & \beta_2 & 0 \\ \sigma^2\beta N_{t+1}^2 & \beta_1 N_{t+1}^2 & \beta_2 N_{t+1}^2 & 0 \\ \kappa\Delta + \sigma^2\beta\sqrt{\Delta}N_{t+1} & \beta_1\sqrt{\Delta}N_{t+1} & \beta_2\sqrt{\Delta}N_{t+1} & \phi \end{bmatrix} \begin{bmatrix} 1 \\ \sigma_t^2 \\ Y_t^2 \\ \log \tilde{Z}_t \end{bmatrix}$$

Figure 5.5 depicts the sample paths for the commodity price  $(\tilde{Z}_t)_{t=0}^T$  for parameters:  $\tilde{Z}_0 = 0.4$ ,  $\phi = 1$  and  $0.6$ ,  $\kappa = 0.05$ ,  $\beta_1 = 0.8$ ,  $\beta_2 = 0.1$ ,  $\sigma^2 = \sigma_0^2 = \sqrt{0.08}$  and  $Y_0^2 = 1$ . The left plot shows the sample paths when there is no mean reversion i.e.  $\phi = 1$  while the right contains mean reversion i.e.  $\phi = 0.6$ . The behaviour of the prices are clearly very different. Since the logarithmic commodity price is now contained in the fourth component  $z^{(4)}$  of the state vector  $z = (z^{(i)})_{i=1}^4$ , we adjust the cash flow function as

$$h_t(z) = 5\Delta \exp(z^{(4)}) \exp(-(r + \zeta)t\Delta) - 2.5\Delta \exp((\rho - r - \zeta)t\Delta).$$

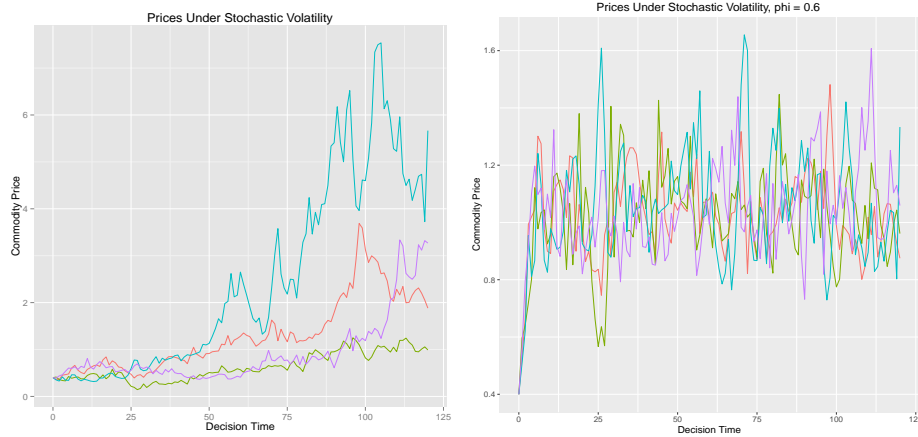


Figure 5.5: Sample paths for  $(\tilde{Z}_t)_{t=0}^T$  under no mean reversion (left) and mean reversion (right)

In the previous examples we have used equally spaced grids. However, for this four dimensional state space we generate the so-called stochastic grid using clustering of a point cloud which we obtain from several Monte Carlo runs of the sample paths simulations. Such grid generation procedure is appropriate for problems involving high dimensional state spaces. The primal and dual values in Table 5.5 were generated using a 2,000 point stochastic grid starting from  $(1, \sqrt{0.08}, 1, \log(0.4))$ , while the stochastic grid itself was generated using 1,000 sample paths. The primal and dual values were generated using  $K = 500$  paths and  $I = 500$  sub-simulations. The Table 5.5 contains the upper and lower bounds for the value of the commodity reserve for  $\beta_1 = 0.8$ ,  $\beta_2 = 0.1$  and  $Y_0^2 = 1$ . These values were computed using 10,000 point disturbances discretization based on equidistant quantiles of the standard normal.

Table 5.5 also clearly shows that bounds are less accurate for higher values of  $\phi$  due to lack of concentration due to weaker mean reversion. A more dense grid and a larger sample of the disturbances should yield more accurate results.

Table 5.5: Resource Valuation Under Stochastic Volatility

$\phi$	$\tilde{Z}_0$	Opened Resource		Closed Resource	
		Primal	Dual	Primal	Dual
1	0.3	3.4337(.1069)	4.4240(.4663)	3.6337(.1069)	4.6240(.4663)
	0.4	7.5215(.2035)	8.8880(.6060)	7.7215(.2035)	9.0878(.6060)
	0.5	12.7777(.6901)	13.8656(.7422)	12.9777(.6901)	14.0614(.7422)
0.8	0.3	6.5229(.0109)	6.5372(.0152)	6.5232(.0110)	6.5376(.0152)
	0.4	7.4872(.0112)	7.5005(.0153)	7.3028(.0112)	7.3166(.0153)
	0.5	8.3380(.0120)	8.3512(.0159)	8.1380(.0120)	8.1513(.0159)
0.6	0.3	7.7928(.0052)	7.7960(.0058)	7.7262(.0052)	7.7294(.0059)
	0.4	8.2726(.0051)	8.2759(.0057)	8.0755(.0051)	8.0788(.0057)
	0.5	8.6992(.0051)	8.7024(.0058)	8.4992(.0051)	8.5024(.0058)

Resource valuation where  $\kappa = 0.05$ ,  $\beta_1 = 0.8$ ,  $\beta_2 = 0.1$ ,  $\sigma_0^2 = \sqrt{0.08}$  and  $Y_0^2 = 1$ . The standard errors are given in the paranthesis.

## 6 Conclusion

This paper represents a first application of pathwise approach to dynamic programming in the area of commodity resource valuation and extraction. Our study shows that high-quality solutions can be obtained with low computational efforts for realistic applications. By representing the extraction problem as a convex stochastic switching problem in discrete time, this paper has demonstrated that accurate and helpful practical insights can be deduced from approximate numerical solutions. Due to a standardized problem formulations, other situations can easily be adopted and our concepts can be generalized and extended to other application areas of optimal stochastic switching.

## References

- [1] L. Andersen and M. Broadie. Primal-dual simulation algorithm for pricing multidimensional american options. *Management Science*, 50(9):1222–1234, 2004.
- [2] E. Bayraktar and M. Egami. On the one-dimensional optimal switching problem. *Mathematics of Operations Research*, 35(1):140–159, 2010.
- [3] T. Boomsma, N. Meade, and S. Fleten. Renewable energy investments under different support schemes : a real options approach. *European Journal of Operational Research*, 220(1):225–237, 2012.
- [4] M. Brennan and E. Schwartz. Evaluating natural resource investments. *The Journal of Business*, 58(2):135–57, 1985.
- [5] D. Brown, J. Smith, and P. Sun. Information relaxations and duality in stochastic dynamic programs. *Operations Research*, 58(4):785–801, 2010.
- [6] R. Carmona and M. Ludkovski. Valuation of energy storage: an optimal switching approach. *Quantitative Finance*, 10(4):359–374, 2010.
- [7] J. Hinz. Optimal stochastic switching under convexity assumptions. *SIAM Journal on Control and Optimization*, 52(1):164–188, 2014.



- [8] J. Hinz and N. Yap. Algorithms for optimal control of stochastic switching systems. *Theory of Probability and its Applications*, (4):770–800, 2015.
- [9] N. Meinshausen and B. Hambly. Monte carlo methods for the valuation of multiple-exercise options. *Mathematical Finance*, 14(4):557–583, 2004.
- [10] R. Paschke and M. Propkopczuk. Commodity derivatives valuation with autoregressive and moving average components in the price dynamics. *Journal of Banking and Finance*, 34(1):2742–2752, 2010.
- [11] M. Puterman. *Markov Decision Processes: Discrete Stochastic Dynamic Programming*. Wiley, New York, 1994.
- [12] L. Rogers. Pathwise stochastic optimal control. *SIAM J. Control Optimisation*, 46(3):1116–1132, 2007.
- [13] S. Sarkar. The effect of mean reversion on investment under uncertainty. *Journal of Economic Dynamics and Control*, 28(2):377–396, 2003.
- [14] E. Schwartz. The stochastic behavior of commodity prices: Implications for valuation and hedging. *The Journal of Finance*, 52(3):923–973, 1997.
- [15] A. Tsekrekos. The effect of mean reversion on entry and exit decisions under uncertainty. *Journal of Economic Dynamics and Control*, 34(4):725–742, 2010.
- [16] A. Tsekrekos, M. Shackleton, and R. Wojakowski. Evaluating natural resource investments under different model dynamics: managerial insights. *European Financial Management*, 18(4):543–577, 2012.
- [17] A. Tsekrekos and A. Yannacopoulos. Optimal switching decisions under stochastic volatility with fast mean reversion. *European Journal of Operational Research*, 251(1):148–157, 2016.